



This is a pre- or post-print of an article published in

**Salomon, J.J., Gausterer, J.C., Yahara, T., Hosoya, K.-
I., Huwer, H., Hittinger, M., Schneider-Daum, N., Lehr,
C.-M., Ehrhardt, C.**

**Organic cation transporter function in different in vitro
models of human lung epithelium**

**(2015) European Journal of Pharmaceutical Sciences, 80,
pp. 82-88.**

For publication in:

European Journal of Pharmaceutical Sciences

Organic cation transporter function in different *in vitro* models of human lung epithelium

Johanna J. Salomon^{1,§}, Julia C. Gausterer¹, Tohru Yahara², Ken-ichi Hosoya², Hanno Huwer³, Marius Hittinger⁴, Nicole Schneider-Daum⁴, Claus-Michael Lehr⁴, Carsten Ehrhardt^{1,*}

¹School of Pharmacy and Pharmaceutical Sciences and Trinity Biomedical Sciences Institute, Trinity College Dublin, Dublin, Ireland

²Graduate School of Medicine and Pharmaceutical Sciences, University of Toyama, Toyama, Japan

³Department of Cardiothoracic Surgery, Völklingen Heart Centre, Völklingen, Germany

⁴Drug Delivery, Helmholtz Institute for Pharmaceutical Research Saarland (HIPS), Helmholtz Centre for Infection Research, Saarbrücken, Germany

[§]Current address: Department of Translational Pulmonology, Translational Lung Research Center (TLRC), Member of the German Center for Lung Research (DZL), University of Heidelberg, Heidelberg, Germany

***Corresponding author**

Dr. Carsten Ehrhardt, School of Pharmacy and Pharmaceutical Sciences, Trinity College Dublin, Dublin 2, Ireland, tel.: +353-1-896-2441, email: ehrhardc@tcd.ie

Abstract

Organic cation transporters (OCT) encoded by members of the solute carrier (SLC) 22 family of genes are involved in the disposition of physiological substrates and xenobiotics, including drugs used in the treatment of chronic obstructive lung diseases and asthma. The aim of this work was to identify continuously growing epithelial cell lines that closely mimic the organic cation transport of freshly isolated human alveolar type I-like epithelial cells (ATI) in primary culture, and which consequently, can be utilised as *in vitro* models for the study of organic cation transport at the air-blood barrier. OCT activity was investigated by measuring [¹⁴C]-tetraethylammonium (TEA) uptake into monolayers of Calu-3, NCI-H441 and A549 lung epithelial cell lines in comparison to ATI-like cell monolayers in primary culture. Levels of time-dependent TEA uptake were highest in A549 and ATI-like cells. In A549 cells, TEA uptake had a saturable and a non-saturable component with $K_m = 528.5 \pm 373.1 \mu\text{M}$, $V_{\text{max}} = 0.3 \pm 0.1 \text{ nmol/min/mg protein}$ and $K_d = 0.02 \mu\text{l/min/mg protein}$. TEA uptake into Calu-3 and NCI-H441 cells did not reach saturation within the concentration range studied. RNAi experiments in A549 cells confirmed that TEA uptake was mainly facilitated by OCT1 and OCT2. Co-incubation studies using pharmacological OCT modulators suggested that organic cation uptake pathways share several similarities between ATI-like primary cells and the NCI-H441 cell line, whereas more pronounced differences exist between primary cells and the A549 and Calu-3 cell lines.

Keywords: Lung epithelial cell lines; OCT1; OCT2; OCT3; pulmonary drug disposition

1. Introduction

The membranous transport of several physiological regulators of pulmonary cell function and lung fluid homeostasis has been suggested to be facilitated by members of the organic cation transporter (OCT) family encoded by the *SLC22A1-A3* genes (Salomon and Ehrhardt, 2012). In mammals, OCT1, OCT2 and OCT3 translocate small (i.e. < 500 Da) organic cations with broad, overlapping affinities for endogenous substrates, such as choline, acetylcholine and monoamine neurotransmitters, as well as a variety of xenobiotics (Pelis and Wright, 2014). OCTs operate electrogenically and independent of sodium gradients and transport in both directions following the substrates' concentration gradient (Ciarimboli, 2010; Koepsell et al., 2007). OCT physiology in tissues such as the liver, gut and kidneys has by and large been well characterised (Nies et al., 2011), nonetheless, the lungs remain somewhat understudied in this regard. Moreover, OCT expression data concerning the respiratory epithelium is often limited to gene or PCR-based *in vitro* studies (Bleasby et al., 2006; Courcot et al., 2012; Endter et al., 2009; Mukherjee et al., 2012) and only a small number of reports show OCT immunocytochemistry or indeed transporter function (Lips et al. 2005; Macdonald et al., 2013; Nakanishi et al., 2013). Very recently, it has been shown by our group that β_2 agonists interact with OCT at the lung epithelium (Salomon et al., 2015), however, the clinical relevance of these findings are not fully understood to date.

One confounding factor for this scarcity of data is the limited availability of appropriate *in vitro* models for the study of ion and solute transport in the human distal lungs (Kim et al., 2001). Whilst freshly isolated human alveolar or

bronchiolar epithelial cells in primary culture remain the gold standard for any kind of transport study involving the respiratory zone, limited availability of tissue, ethical restraints in certain countries and often economical and/or logistical shortcomings, hamper the use of human tissue. Accordingly, a number of cell lines has been utilised in ion and solute transport experiments, focusing on the respiratory epithelium, including the adenocarcinoma cell line, A549 (Sporty et al., 2008). Although A549 cells have been used as an *in vitro* model by many investigators, it should be noted that this cell line does not form tight monolayers of polarised cells (Forbes and Ehrhardt, 2005), an essential feature for transmonolayer transport studies. The cell lines 16HBE14o-, VA10, Nuli-1 and Calu-3, all of trachea-bronchial epithelial origin, have functional tight junctions and thus generate reasonable transepithelial electrical resistance (TEER) values indicative of polarised mucosal barriers (Buckley et al., 2011). The cell line NCI-H441 also forms tight monolayers and exhibits features of both alveolar (i.e. type II cell) and bronchiolar (i.e. club cell) epithelial phenotype (Hermanns et al., 2005; Salomon et al., 2014).

It was the aim of this study to determine OCT activity in a number of commonly used cell lines of human respiratory epithelial origin and to compare the obtained data to freshly isolated human alveolar epithelial cells in primary culture, in order to identify a suitable *in vitro* model for biopharmaceutical and physiological organic cation transport studies at the air-blood barrier.

2. Methods

2.1. Materials

[Ethyl-1-¹⁴C] tetraethylammonium chloride (TEA; 55 mCi/mmol) was purchased from American Radiolabeled Chemicals (Herts, UK). Unlabelled TEA, amantadine, corticosterone, 1,1-diethyl-2,2-cyanine (decynium-22), 1-methyl-4-phenylpyridinium (MPP⁺), verapamil and all cell culture media and supplements were obtained from Sigma-Aldrich (Dublin, Ireland). Quinidine was bought from Santa Cruz Biotechnology (Heidelberg, Germany). All cell culture plastics were purchased from Greiner BioOne (Frickenhausen, Germany).

2.2. Cell line culture

A549 cells (American Type Culture Collection, ATCC CCL-185) were obtained from the European Collection of Animal Cell Cultures (Salisbury, UK). Calu-3 (ATCC HTB-55) and NCI-H441 (ATCC HTB-174) cells were purchased from LGC Promochem (Teddington, UK).

Cell lines were cultured at the following seeding densities: 40,000 cells/cm² (A549; passage numbers 65 - 75), 75,000 cells/cm² (Calu-3; passage numbers 48 - 55) and 100,000 cells/cm² (NCI-H441; passage numbers 55 - 68). A549 cells were grown in Dulbecco's modified Eagle's medium/Ham's F-12 (1:1 mix) (DMEM/F12) supplemented with 5% foetal bovine serum (FBS), 100 U/ml penicillin and 100 µg/ml streptomycin. Calu-3 cells were cultured in minimum essential medium (MEM) supplemented with 10% FBS, 1% non-essential amino acids solution, 1% sodium pyruvate solution, 0.5% glucose solution and 100 U/ml penicillin and 100 µg/ml streptomycin. NCI-H441 cells were cultured in tissue culture flasks using Roswell Park Memorial Institute (RPMI) 1640

medium supplemented with 5% FBS, 1% sodium pyruvate solution, 100 U/ml penicillin and 100 µg/ml streptomycin. Twenty-four hours post-seeding in well plates, this medium was further supplemented with dexamethasone (100 nM) and insulin-transferrin-sodium selenite (ITS) solution (Roche Diagnostics Limited, West Sussex, UK). All cell lines were maintained at 37°C in 5% CO₂ atmosphere and the culture media were exchanged every other day.

2.3. Human alveolar epithelial cell isolation and culture

The use of human tissue specimens was approved by Saarland State Medical Board (Saarbrücken, Germany). Human alveolar type II epithelial cells were isolated according to a protocol modified from Demling *et al.* from non-tumour lung tissue obtained from patients undergoing lung surgery (Demling *et al.*, 2006; Daum *et al.*, 2012). Purified type II cells were seeded at a density of 600,000 cells/cm² on collagen/fibronectin-coated plastics using complete small airways growth medium (SAGM; Lonza, Verviers, Belgium) supplemented with 1% FBS, 100 U/ml penicillin and 100 µg/ml streptomycin. Primary cell monolayers were used after transdifferentiation into an alveolar type I-like (ATI-like) phenotype, following at least one week of culture.

2.4. Uptake studies

Cells were grown to confluent monolayers on 24-well plates for at least 5 (A549), 8 (NCI-H441, ATI-like) and 12 (Calu-3) days, respectively, before being used in uptake studies. Uptake experiments using A549 cells were carried out in extra-cellular fluid buffer (ECF; 122 mM NaCl, 3 mM KCl, 0.4 mM KHPO₄, 25 mM NaHCO₃, 1.4 mM CaCl₂, 1.2 mM MgSO₄, 10 mM HEPES and 10 mM D-

glucose, pH 7.4). All other experiments were performed in freshly prepared, bicarbonated Krebs-Ringer buffer (KRB; 116.4 mM NaCl, 5.4 mM KCl, 0.78 mM NaH₂PO₄, 25 mM NaHCO₃, 1.8 mM CaCl₂, 0.81 mM MgSO₄, 15 mM HEPES and 5.55 mM D-glucose, pH 7.4), unless otherwise stated. Both buffer solutions were found not to be significantly different with regards to organic cation uptake (data not shown). Prior to uptake studies, cell monolayers were washed three times with pre-equilibrated ECF or KRB solution. To initiate organic cation uptake, 200 µl of buffer solution containing [¹⁴C]-TEA (10 µM) was added to each well. For time-course analyses, organic cation uptake was studied over 30 min. To determine concentration dependency and (self)-inhibitory effects on organic cation uptake, cell monolayers were incubated with TEA in the presence of various concentrations (i.e. 0 to 20 mM) of unlabelled compound for 10 min (Calu-3, NCI-H441, ATI-like) or 30 min (A549). In this case, [¹⁴C]-TEA uptake was carried out at 4°C and 37°C and values obtained at 4°C were subtracted from values measured at 37°C in order to account for adsorption and diffusion processes. In all studies a concentration of 10 µM [¹⁴C]-TEA was used. Uptake of TEA was also performed in the presence of several modulators of organic cation transporter function (i.e. amantadine, corticosterone, decynium-22, MPP⁺, quinidine and verapamil).

At the relevant time points, the uptake was stopped by washing cell monolayers three times with ice-cold buffer and 400 µl of 1N NaOH was added to permeabilise the cells for at least 12 h, before 400 µl of 1N HCl was used for neutralisation of the cell lysate. Five-hundred microlitres of lysate was used to measure the cell-associated radioactivity in a liquid scintillation counter (Tri Carb TR2100 Packard Scintillation Counter, Dublin, Ireland). In parallel, the

total cell protein content was quantified using a DC Protein Assay kit (Bio-Rad, Hemel Hempstead, UK) according to the manufacturer's instructions.

2.5. RNA interference studies

A549 cells were seeded in 24-well cell culture plates and grown for 24 h. Two microliters of HyperFect reagent (Qiagen, West Sussex, UK), 50 μ l of DMEM/F12 and siRNA against OCT1, OCT2 or OCT3 (75 nM; Santa Cruz Biotechnology) or scrambled control siRNA (AllStars, Qiagen) were mixed, incubated at room temperature for 5 - 10 min and added drop wise to the cells. The concentrations were chosen according to the manufacturer's guidance and did not cause significant toxicity after transfection with any of the siRNA types. Cells were then incubated at 37°C for 24 h, before the medium was changed back to the standard cell culture medium. After 24, 48 and 72 h, cell monolayers were lysed in cell extraction buffer containing protease inhibitors (Invitrogen, Karlsruhe, Germany). Protein sample concentration was determined with the DC Protein Assay kit and used for Western blot analysis. Uptake studies were carried out with cells after 4 days of culture, i.e. 72 h post transfection.

2.6. Immunoblotting

Lysis of A549 cells was performed on ice in cell extraction buffer (Invitrogen) containing protease inhibitors (Sigma-Aldrich). Cell samples were sonicated twice for 10 s and then the lysate was centrifuged (10,000g at 4°C) for 20 min. The total protein amount was determined by DC Protein Assay kit using bovine serum albumin (BSA) as standard. Samples were standardised to equal protein concentrations, loading buffer was added and the mixture was heated up to

95°C for 5 min, before samples were loaded onto SDS gels. Polyacrylamide gel electrophoresis was performed at 120 V, followed by transfer onto immunoblot polyvinylidene fluoride membranes (Bio-Rad) at 25 V for 30 min. Blots were blocked in washing buffer containing 5% (w/v) BSA for at least one hour at room temperature. Membranes were then incubated with the relevant polyclonal rabbit anti-OCT1, anti-OCT2 or anti-OCT3 antibodies (all from Sigma-Aldrich; dilutions used were 1:200 for OCT1, 1:500 for OCT2 and 1:2000 for OCT3) in washing buffer containing 5% (w/v) BSA. After washing with PBS, the secondary anti-rabbit antibody (1:12,500; Promega, Medical Supply Company, Dublin, Ireland) was added for 1 h at room temperature. Peroxidase activity was detected with Immobilon Western Chemiluminescent HRP substrate (Millipore, Carrigtwohill, Ireland). Signals were documented using a ChemiDoc system (Bio-Rad).

2.7. Data analysis

The uptake of [¹⁴C]-TEA by human respiratory epithelial cells was expressed as the cell-to-medium (cell/medium) ratio calculated by the following equations:

$$\text{Cell/medium ratio} = \frac{[\text{^{14}C}] \text{ dpm per mg cell protein}}{[\text{^{14}C}] \text{ dpm per ml buffer}}$$

[Eq. 1]

The time-dependent uptake was fitted using GraphPad Prism 5. One binding site was assumed and fitting was corrected for non-specific binding.

To calculate the kinetic parameters of TEA uptake, the initial uptake rates were fitted to Equation 2 by means of non-linear least-squares regression analysis using WinNonlin (Pharsight, Sunnyvale, CA).

$$v = V_{\max} \times s / K_m + s$$

[Eq. 2]

where v is the initial uptake rate of the substrate (nmol/min×mg protein), s is the substrate concentration in the medium (μM), K_m is the Michaelis-Menten constant (μM), and V_{\max} is the maximum uptake rate (nmol/min×mg protein).

Results are expressed as means \pm SD unless otherwise stated. Statistical significance of differences between groups was determined by one-way analysis of variance (ANOVA), followed by the modified Fisher's least squares difference method. All experiments were carried out at least in triplicate.

3. Results

3.1. Time course of TEA uptake

The time courses of TEA uptake into human lung epithelial cell monolayers is shown in Figure 1. In ATI-like cells, the cell/medium ratio levelled off after 10 min of incubation and reached a maximal value of $6.08 \pm 1.84 \mu\text{l/mg protein}$ after 30 min (Fig. 1a). Similar trends were observed in NCI-H441 (Fig. 1c) and Calu-3 (Fig. 1d) cells, albeit the maximum cell/medium ratios at 30 min were significantly lower at $1.78 \pm 0.30 \mu\text{l/mg protein}$ and $1.03 \pm 0.08 \mu\text{l/mg protein}$, respectively. TEA uptake was found to be linear in the case of A549 cells (Fig. 1b), reaching a cell/medium ratio of $8.40 \pm 1.43 \mu\text{l/mg protein}$ after 30 min.

3.2. Kinetic analysis of TEA uptake

In A549 cell monolayers, TEA uptake was, at least partially, saturable (Fig. 2a). Eadie-Hofstee transformation of these data (Fig. 2d) indicated a substantial saturable component with $K_m = 528.5 \pm 373.1 \mu\text{M}$ and $V_{\text{max}} = 0.3 \pm 0.1 \text{ nmol/min/mg protein}$. The non-saturable uptake component had a K_d value of $0.02 \mu\text{l/min/mg protein}$, suggesting a minor contribution to the TEA uptake into A549 cells (Fig. 2d). On the contrary, when TEA uptake was studied in NCI-H441 and Calu-3 epithelial monolayers, no saturation was observed in the concentration range studied (Fig. 2b, c).

3.3. RNA interference studies in A549 cells

To investigate the molecular identity of the transporter(s) involved in TEA uptake at the air-blood barrier, knockdown of OCT1, OCT2 and OCT3 cells was carried out in A549 using transporter-specific siRNA. Uptake studies were

performed 3 days post transfection and in parallel, protein expression levels were determined from the same batches of cells (see Supplemental Figure). All experiments were performed in untreated, mock-transfected and OCT siRNA-transfected A549 cells. No significant differences in transporter expression and TEA uptake were observed between untreated and mock-transfected A549 cells (data not shown). OCT protein levels were reduced by approximately 30% (OCT1), 85% (OCT2) and 45% (OCT3), in comparison to the relevant mock-transfected controls (Fig. 3a-c). As shown in Fig. 3d-f, RNAi targeting OCT1 and OCT2 significantly inhibited TEA uptake to $52.5 \pm 3.2\%$ and $50.4 \pm 8.6\%$, respectively, whereas knockdown of OCT3 had a much less pronounced effect of $84.6 \pm 8.3\%$.

3.4. Effect of pharmacological OCT inhibition on TEA uptake

Several different modulators of OCT activity were chosen according to their inhibitory potential (Nies et al., 2011) and their effects were corrected for non-specific binding at 4°C (Fig. 4).

Amantadine (1 mM) only marginally inhibited TEA uptake into ATI-like cells (i.e. $85.8 \pm 14.5\%$ of control), whereas in A549 cells, uptake was reduced to $24.6 \pm 1.8\%$ of control. In NCI-H441 and Calu-3 values of $50.8 \pm 32.9\%$ and $57.4 \pm 15.0\%$ were obtained (Fig. 4a). The effect of corticosterone (500 µM) on ATI-like cells was much more pronounced (i.e. $19.3 \pm 10.2\%$); a value comparable to what was seen in A549 cells (i.e. $12.5 \pm 1.8\%$). NCI-H441 and Calu-3 cells were less affected by the steroid, with TEA uptake being reduced to $57.7 \pm 15.9\%$ (NCI-H441) and $44.5 \pm 0.3\%$ (Calu-3) (Fig. 4b). Decynium-22 (500 µM) strongly reduced TEA uptake in ATI-like ($18.6 \pm 9.9\%$), A549 ($0.0 \pm 0.8\%$) and NCI-H441

($6.1 \pm 4.7\%$) cells, whereas no inhibition was measured in Calu-3 cells ($97.0 \pm 26.9\%$) (Fig. 4c). Very similar effects were noticed when quinidine was used: ATI-like ($1.5 \pm 1.4\%$), A549 ($0.0 \pm 0.8\%$) and NCI-H441 ($7.2 \pm 6.8\%$) cells showed almost complete inhibition of TEA uptake and Calu-3 cells ($96.6 \pm 7.3\%$) were not affected (Fig. 4e). MPP⁺ (1 mM) caused a strong reduction in TEA taken up by ATI-like ($33.9 \pm 14.8\%$), NCI-H441 ($28.6 \pm 9.8\%$) and Calu-3 ($14.6 \pm 6.5\%$) cells. In A549 cells, the effect of MPP⁺ was even more pronounced, lowering TEA uptake to $4.5 \pm 1.2\%$ of control (Fig. 4d). Verapamil (200 μ M) was also a potent inhibitor in all four cell models, completely abolishing TEA uptake to $0.0 \pm 0.4\%$ and $0.0 \pm 11.8\%$ in A549 and NCI-H441 cells, respectively. TEA accumulation into ATI-like cells was somewhat less affected ($15.7 \pm 10.8\%$) as it was in Calu-3 cells ($16.6 \pm 2.3\%$) (Fig. 4f).

In general, when comparing the pharmacological inhibition profiles in the three cell lines with what was observed in the primary cell cultures, significant ($P < 0.05$) differences were detected for 4 inhibitors (i.e. amantadine, Dec-22, MPP⁺ and verapamil) in the case of A549 cells, 3 inhibitors (i.e. corticosterone, Dec-22 and quinidine) in the case of Calu-3 cells and only one compound (i.e. corticosterone) was deviant in the case of NCI-H441 cells.

4. Discussion

Studying the contribution of membrane transporters to the (patho)physiology, pharmacokinetics and pharmacodynamics in a complex organ such as the lungs is a formidable task, and data generated in robust *in vitro* models are invaluable. Membrane transporters have been confirmed to be present throughout the different areas of lung mucosa (Gumbleton et al., 2011), however, only a limited number of activity studies have been carried out in human pulmonary epithelial cells thus far. To worsen the situation, most studies have utilised dissimilar *in vitro* models (Horvath et al., 2007; Macdonald et al., 2013; Mukherjee et al., 2012; Salomon et al., 2012). There is thus, an urgent demand for physiologically relevant and well-characterised *in vitro* models of human lung epithelium for studies of pulmonary solute transport, e.g. in the context of drug disposition.

In this work, we sought to determine OCT activity in a number of commonly used cell lines of human respiratory epithelial origin (i.e. A549, NCI-H441 and Calu-3) and to compare the data thus obtained to freshly isolated human alveolar epithelial cells in primary culture, in order to establish which – if any – of these cell lines offers the highest level of similarity.

In previous studies, 4-[4-(dimethylamino)styryl]-1-methylpyridinium iodide (ASP⁺), a cationic fluorescent dye, was used by us and others as probe for OCT-mediated transport (Horvath et al., 2011; Macdonald et al., 2013; Salomon et al., 2012; Stachon et al., 1997). However, ASP⁺ is lacking specificity as an OCT substrate in organotypic cell models that express a gamut of transporter types. The compound, e.g. is also a high affinity ligand of monoamine

transporter such as NET, DAT and SERT (). and K_m values reported for ASP⁺ in heterologous systems over-expressing monoamine transporters were about 1000-times lower than those measured in OCT transfectants (Nies et al., 2011; Haunsø and Buchanan, 2007; Mason et al., 2005; Oz et al., 2010). Hence, in this study, TEA was used, which appears to be somewhat less promiscuous (Nies et al., 2011).

TEA uptake increased in a time-dependent manner in all investigated cell models. Human alveolar epithelial cells in primary culture and A549 cell monolayers exhibited considerable higher uptake rates than NCI-H441 cells, which in turn showed higher uptake than Calu-3 cells. Kinetic analysis of TEA uptake by A549 cells revealed the presence of a transport system with a saturable and a non-saturable site. The estimated K_m for the linear component of TEA uptake (529 μM) was in the same order of magnitude as those reported for hOCT1 (168 and 229 μM) in HeLa cells (Zang et al., 1997; Bednarczyk et al., 2003), hOCT2 (76 and 431 μM) and hOCT3 (1372 μM) in *Xenopus laevis* oocytes (Gorboulev et al., 2007; Bourdet et al., 2005). A K_m of 436 μM for TEA was determined in OCTN1-transfected HEK-293 cells by Tamai and co-workers (Tamai et al., 1997). This low-affinity uptake of TEA in A549 cells was significantly decreased by several OCT1-3 substrates such as corticosterone, decynium-22 or MPP⁺. Amantadine (OCT2 inhibitor) reduced TEA uptake by about 70% of the control value. Kinetic analysis of TEA uptake in NCI-H441 and Calu-3 cells showed a strong, non-saturable component in the concentration range used.

RNAi studies in A549 cells resulted in significantly reduced TEA uptake activity when OCT1 and OCT2 were silenced, whereas knockdown of OCT3 had almost no effect. Regrettably, RNAi studies using primary alveolar epithelial cells did not produce meaningful data due to the high toxicity of the transfection reagent (data not shown).

As an alternative, pharmacological inhibitors were used to deconvolve and compare cation uptake pathways in the different cell types. ATI-like cells were least affected by amantadine (OCT1 and OCT2 inhibitor), whereas corticosterone, Dec-22, MPP⁺, quinidine and verapamil, which are all known to block all three OCT subtypes, showed inhibitory effects of 70-95% of TEA uptake (MPP⁺ < corticosterone = Dec-22 < verapamil < quinidine).

OCT expression pattern determined by Western blot (Salomon et al. 2012; Salomon et al., 2014) and the now studied TEA uptake rate were quite similar in ATI-like and A549 cells. Nevertheless, were the highest number of significantly different pharmacological effects on TEA uptake observed when comparing the two cell types. ATI-like cells were generally less affected by the modulators than A549. It can thus, be hypothesised that organic cation transporters are either expressed at a lower level and/or on the basolateral membranes of the primary cells, which would make them less accessible for both substrates and inhibitors (Salomon et al., 2012). Inhibition of TEA uptake into Calu-3 cells was also significantly different from what was observed in ATI-like cells in the case of half of the pharmacological inhibitors studied; specifically, corticosterone, Dec-22 and quinidine proved to be less effective in Calu-3 than in primary alveolar epithelial cells. Moreover, TEA accumulation in Calu-3 was only a fraction of values measured in ATI-like cells. Recent studies have confirmed that OCT2 is

absent in Calu-3 cells (Macdonald et al., 2013; Mukherjee et al., 2012; Salomon et al., 2012), suggesting that OCT1 might play a key role in translocating organic cations in this cell type.

When comparing data from ATI-like monolayers with those from NCI-H441 cells, it was noted that, albeit TEA uptake over time was lower in the cell line, there was only one outlier observed in the inhibitor studies (i.e. corticosterone). Considering that expression patterns of OCT between the two cell types were very close when assessed with molecular biological techniques (Salomon et al., 2014), NCI-H441 epithelial cells seem to exhibit profound similarities to primary cells in their spatial expression and organic cation transporter function.

5. Conclusions

Uptake pathways for cations in A549 and Calu-3 cells and ATI-like cells are very different from each other, whereas a higher degree of similarity was observed between primary calls and the NCI-H441 cell line. Organic cation uptake at the lung epithelial barrier, nevertheless, very likely also involves other transporters not studied in this paper such as gene products encoded by *SLC5*, *SLC6*, *SLC7*, *SLC29*, *SLC44* and *SLC47*.

Acknowledgements

This work has been funded in parts by a Strategic Research Cluster grant (07/SRC/B1154) under the National Development Plan co-funded by EU Structural Funds and SFI.

References

- Bleasby, K. et al., 2006. Expression profiles of 50 xenobiotic transporter genes in humans and pre-clinical species: a resource for investigations into drug disposition. *Xenobiotica* 36(10-11):963-988.
- Buckley, S.T. et al., 2011. In vitro cell culture models for evaluating controlled release pulmonary drug delivery. In: Smyth H, Hickey AJ (Ed) *Controlled Release Science and Technology: Pulmonary Drug Delivery*. Springer, New York, pp 417-42.
- Ciarimboli, G., 2010. Organic cation transporters. *Xenobiotica* 38: 936-71.
- Courcot, E. et al., 2010. Xenobiotic Metabolism and Disposition in Human Lung Cell Models: Comparison with In Vivo Expression Profiles. *Drug Metab. Dispos.* 40(10):1953-65.
- Daum, N. et al., 2012. Isolation, cultivation, and application of human alveolar epithelial cells. *Methods Mol. Biol.* 806:31-42.
- Demling, N. et al., 2006. Promotion of cell adherence and spreading: a novel function of RAGE, the highly selective differentiation marker of human alveolar epithelial type I cells. *Cell Tissue Res.* 323(3):475-88.
- Endter, S. et al., 2009. RT-PCR analysis of ABC-, SLC- and SLCO-drug transporters in human lung epithelial cell models. *J. Pharm. Pharmacol.* 61(5):583-591.
- Forbes, B., Ehrhardt, C., 2005 Human respiratory epithelial cell culture for drug delivery applications. *Eur. J. Pharm. Biopharm.* 60:2:193-205.

- Gumbleton, M. et al., 2011. Spatial expression and functionality of drug transporters in the intact lung: objectives for further research. *Adv. Drug Deliv. Rev.* 63(1-2):110-8.
- Haunsø, A., Buchanan, D., 2007. Pharmacological characterization of a fluorescent uptake assay for the noradrenaline transporter. *J. Biomol. Screen* 12(3):378-84.
- Hermanns MI, Unger RE, Kehe K, Peters K, Kirkpatrick CJ (2004) Lung epithelial cell lines in coculture with human pulmonary microvascular endothelial cells: development of an alveolo-capillary barrier in vitro. *Lab Invest.* 84(6):736-52.
- Horvath, G. et al., 2007. Epithelial organic cation transporters ensure pH-dependent drug absorption in the airway. *Am. J. Respir. Cell Mol. Biol.* 36:53-60.
- Horvath, G. et al., 2011. Rapid nongenomic actions of inhaled corticosteroids on long-acting $\beta(2)$ -agonist transport in the airway. *Pulm. Pharmacol. Ther.* 24:654-9.
- Kim, K.J. et al., 2001. A useful in vitro model for transport studies of alveolar epithelial barrier. *Pharm. Res.* 18(3):253-5.
- Koepsell, H. et al., 2007. Polyspecific organic cation transporters: structure, function, physiological roles, and biopharmaceutical implications. *Pharm. Res.* 24:1227-51.

- Lips, K.S. et al., 2005. Polyspecific cation transporters mediate luminal release of acetylcholine from bronchial epithelium. *Am. J. Respir. Cell Mol. Biol.* 33(1):79-88.
- Macdonald, C. et al., 2013. Characterization of Calu-3 cell monolayers as a model of bronchial epithelial transport: organic cation interaction studies. *J. Drug Target.* 21(1):97-106.
- Mason, J.N. et al., 2005. Novel fluorescence-based approaches for the study of biogenic amine transporter localization, activity, and regulation. *J. Neurosci. Methods* 143(1):3-25.
- Mukherjee, M. et al., 2012. Evaluation of air-interfaced Calu-3 cell layers for investigation of inhaled drug interactions with organic cation transporters in vitro. *Int. J. Pharm.* 426:7-14.
- Nakanishi, T. et al., 2013. In vivo evidence of organic cation transporter-mediated tracheal accumulation of the anticholinergic agent ipratropium in mice. *J. Pharm. Sci.* 102(9):3373-81.
- Nies, A.T. et al., 2011. Organic cation transporters (OCTs, MATEs), in vitro and in vivo evidence for the importance in drug therapy. *Handb. Exp. Pharmacol.* 201:105-67.
- Oz, M. et al., 2010. Real-time, spatially resolved analysis of serotonin transporter activity and regulation using the fluorescent substrate, ASP⁺. *J. Neurochem.* 114(4):1019-1029.

- Pelis, R.M., Wright, S.H., 2014. SLC22, SLC44, and SLC47 transporters--organic anion and cation transporters: molecular and cellular properties. *Curr. Top. Membr.* 73:233-61.
- Salomon, J.J., Ehrhardt, C., 2012. Organic cation transporters in the blood-air barrier: Expression and implications for pulmonary drug delivery. *Ther. Deliv.* 3:735-7.
- Salomon, J.J. et al., 2012. Transport of the fluorescent organic cation 4-(4-(dimethylamino)styryl)-N-methylpyridinium iodide (ASP⁺) in human respiratory epithelial cells. *Eur. J. Pharm. Biopharm.* 81: 351-9.
- Salomon, J.J. et al., 2014. The cell line NCI-H441 is a useful in vitro model for transport studies of human distal lung epithelial barrier. *Mol. Pharm.* 11(3):995-1006.
- Salomon, J.J. et al., 2015. Beta-2 Adrenergic Agonists Are Substrates and Inhibitors of Human Organic Cation Transporter 1. *Mol Pharm* [Epub ahead of print]
- Sporty, J.L. et al., 2008. In vitro cell culture models for the assessment of pulmonary drug disposition. *Expert Opin. Drug Metab. Toxicol.* 4:333-45.
- Stachon, A. et al., 1997. Characterisation of organic cation transport across the apical membrane of proximal tubular cells with the fluorescent dye 4-Di-1-ASP. *Cell Physiol. Biochem.* 7:265–274.

Figure legends

Fig. 1 Time course of [¹⁴C]-TEA uptake into human ATI-like (a), A549 (b), NCI-H441 (c) and Calu-3 (d) epithelial cells. Uptake of [¹⁴C]-TEA (10 μM) was determined at 37°C for 30 min and data were fitted by means of non-linear regression analysis. Each point represents means ± SD (*n* = 3).

Fig. 2 Concentration dependence of [¹⁴C]-TEA uptake by human respiratory epithelial cell monolayers. Alveolar (A549) cells were incubated for 30 min at concentrations ranging from 0.5 to 20 mM at pH 7.4 (a). [¹⁴C]-TEA total uptake (solid line), saturable component (broken line) and non-saturable component (dotted line) are shown. Furthermore, [¹⁴C]-TEA uptake data was analysed using Eadie-Hofstee transformation in A549 cells (d). In the case of NCI-H441 (b) and Calu-3 (c) cells, [¹⁴C]-TEA uptake was performed for 10 min. Results were obtained by subtraction of [¹⁴C]-TEA uptake at 4°C as the non-specific component from the total uptake. Each point represents means ± SD (*n* = 3).

Fig. 3 RNAi of OCT1-3 in A549 human alveolar epithelial cells. Cells were transfected with siRNA against OCT1, OCT2 and OCT3, and total cell protein was isolated and analysed by Western blotting three days later. Scrambled siRNA was used as control. Densitometric analysis of OCT expression corrected for β-actin is shown in (a, OCT1), (b, OCT2) and (c, OCT3). The functional effect of RNAi was studied by measuring [¹⁴C]-TEA uptake (10 μM) into A549 cell monolayers from the same batch at pH 7.4 and 37°C and shown in (d, OCT1), (e, OCT2) and (f, OCT3). Data represent means ± SD (*n* = 3 - 6).

**** $P < 0.01$ and * $P < 0.05$** indicates a significant difference from mock transfected cells.

Fig. 4 Comparative analysis of inhibitory effects of substrates on [^{14}C]-TEA uptake into ATI-like, A549, NCI-H441 and Calu-3 cell monolayers. [^{14}C]-TEA uptake (10 μM) of was measured after 30 min (A549) and 10 min (ATI-like, Calu-3, NCI-H441) at 37°C and pH 7.4 in the presence of 1 mM amantadine (**a**), 500 μM corticosterone (**b**), 500 μM decynium-22 (**c**), 1 mM MPP⁺ (**d**), 500 μM quinidine (**e**) and 200 μM verapamil (**f**). Values were compared between human alveolar primary cells (ATI-like, white columns) and continuously grown A549 (black columns), NCI-H441 (grey columns) and Calu-3 (dark grey columns) cells. Values were obtained by calculating the difference between uptake at 37°C and 4°C. Data represent means \pm SEM ($n = 6 - 9$). * $P < 0.05$ indicates a significant difference from data obtained with ATI-like monolayers. Please note the differences in y-axis scale.

Figure 1

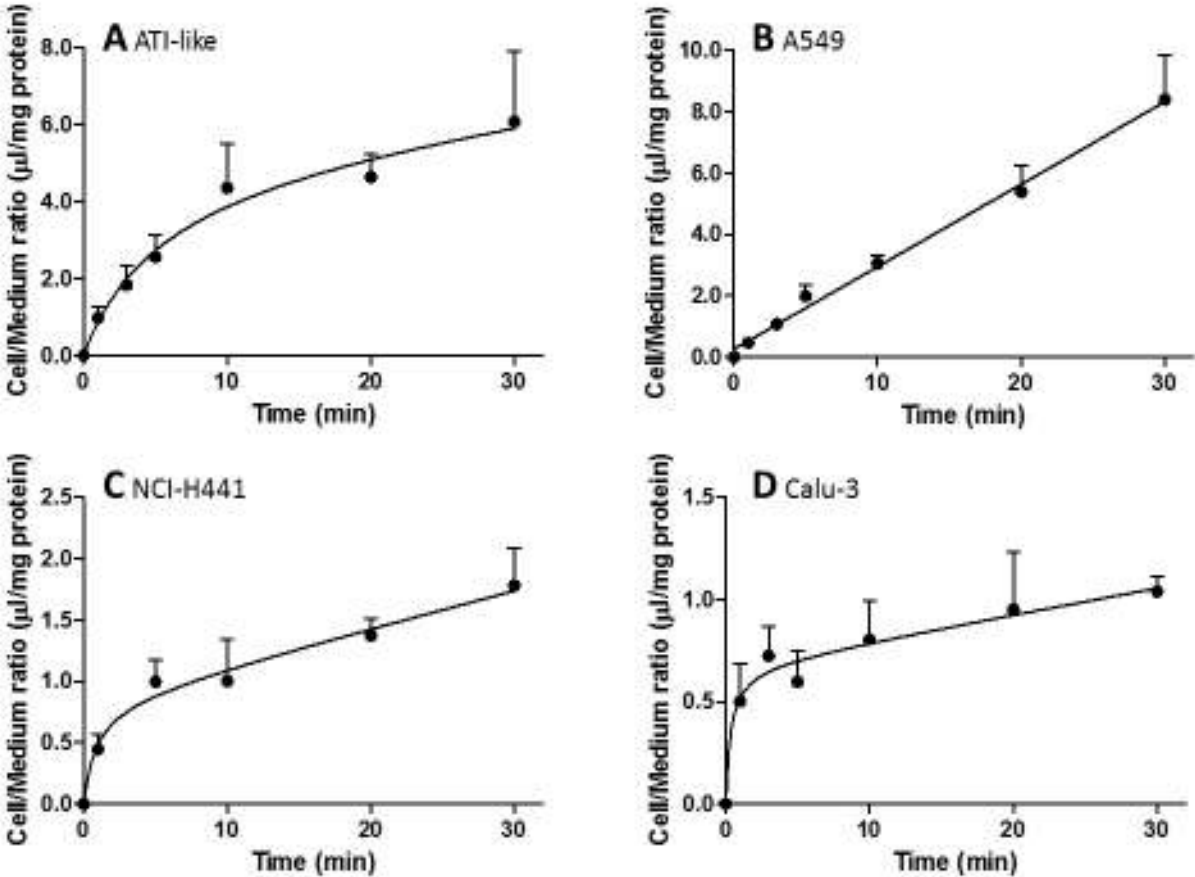


Figure 2

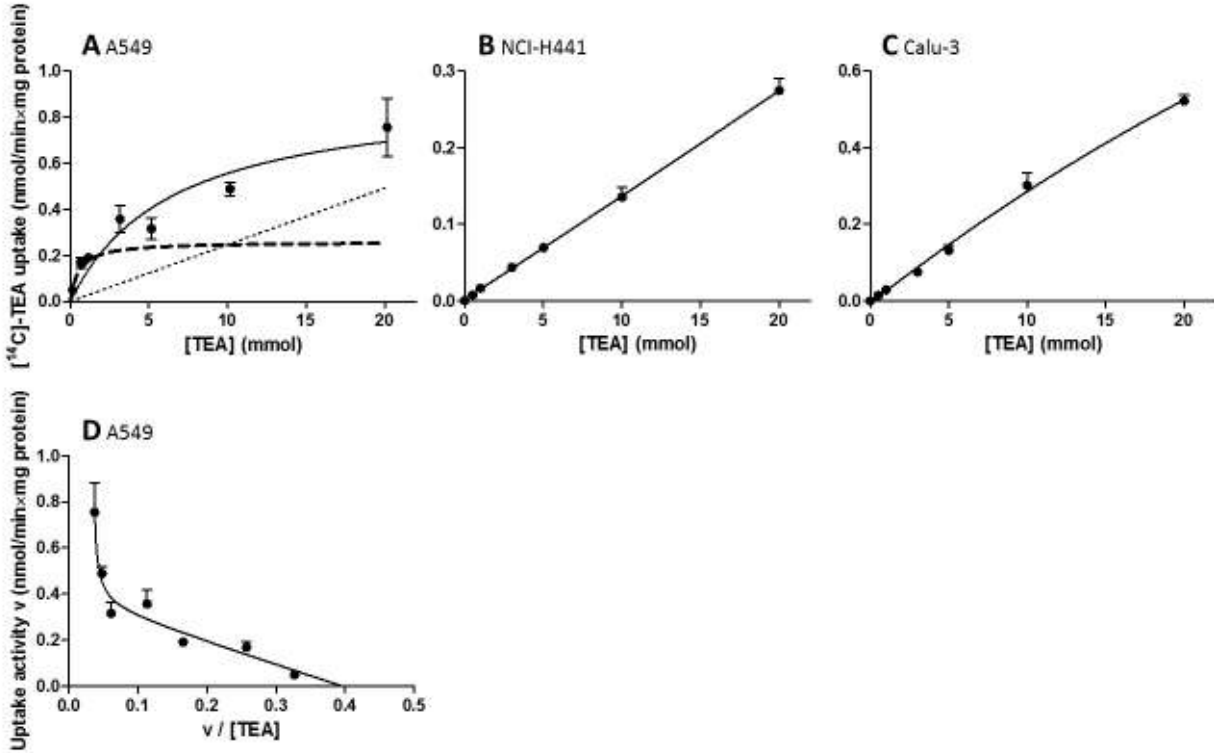


Figure 3

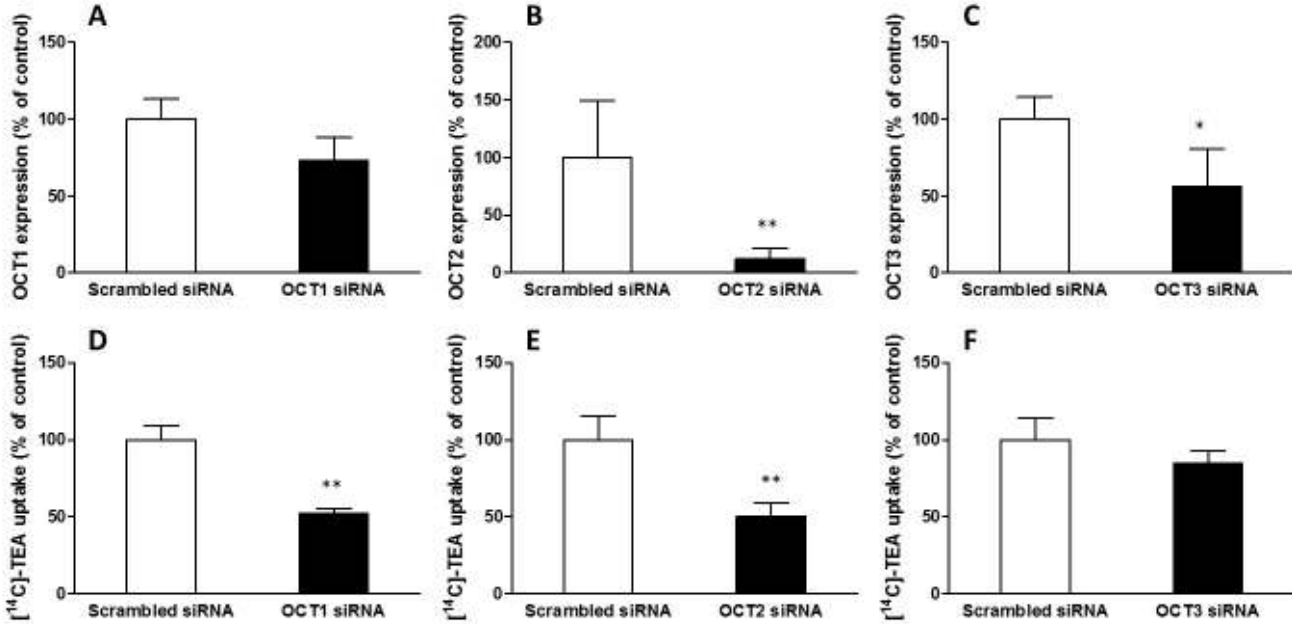


Figure 4

